Dyes and Pigments 92 (2012) 1144–1152

Contents lists available at SciVerse ScienceDirect

Dyes and Pigments

journal homepage: www.elsevier.com/locate/dyepig

Excited-state nature in benzodifuranone dyes: Insights from *ab initio* simulations

José P. Cerón-Carrasco, Alexis Ripoche, Fabrice Odobel, Denis Jacquemin*

Chimie et Interdisciplinarité: Synthèse, Analyse, Modélisation (CEISAM), UMR CNRS 6230, Université de Nantes, 2 rue de la Houssinière – BP 92208, 44322 Nantes cedex 3, France

ARTICLE INFO

Article history:
Received 27 May 2011
Received in revised form
18 July 2011
Accepted 20 July 2011
Available online 17 August 2011

Keywords:
Benzodifuranone
Organic dyes
Strong acceptors
Time-dependent density functional theory
Dye sensitised solar cells (DSSC)
Absorption spectra

ABSTRACT

Using *ab initio* theoretical tools simultaneously accounting for electron correlation and environmental effects, we have simulated the optical spectra of benzodifuranone dyes. In a first step, a valuable computational protocol has been defined and it turned out that a PCM-TD-M06-2X/6-311+G(2d,p)//PCM-PBE0/6-311G(d,p) approach provides an adequate balance between computational requirements and accuracy (deviations of ca. 10 nm with respect to experiment). In a second stage, we have calculated the spectrum of a large series of push-pull structures, and it turned out that the benzodifuranone core is a strong electron capturing group at the excited-state. Indeed, strong auxochroms like the nitro and cyano groups fall short to significantly perturb the LUMO of this series of chromogens. Eventually, in a last phase, the implications of these results are discussed for a series of organic dyes of potential interest for solar cells (DSSC).

1. Introduction

In this work, we investigate the properties of dyes belonging to the benzodifuranone and benzodipyrrolidone families (**I** and **II** in Fig. 1, respectively). Benzodifuranone chromophores may be synthesised by two routes [1–4], the first implying the reaction of hydroquinone with phenylglycolic acid whereas the second uses benzoquinone and cyanoacetic acid as starting materials [1]. Likewise, benzodipyrrolidones may be obtained through the reaction of phenylglycolic acid with paraphenylenediamine derivatives [1,2]. These two series of dyes provide vivid blue and red colours with a very intense visible main absorption band, λ_{max}, spanning over a large window, ca. 450–700 nm depending on the selected auxochroms [2,3]. Interestingly, these dyes have been the subject of only a limited number of investigations from both the theoretical and experimental points of view despite their large potential for practical applications. Indeed, due to their efficient light-harvesting properties, they may be applied not only as disperse dyes [2], or as non-linear optic molecules [4], but also as a central chromophoric unit in more complex architecture such as dyes of potential interest for solar cells (dyes sensitised solar cells, DSSC). The interest for benzodifuranone derivatives is well illustrated by the numerous patents that have been deposited during the last five years [5]. It is therefore important to unravel the nature of the interactions between these chromophores and incoming light in order to pave the way towards their rational optimisation. Of course, such task implies to use tools able to explore electronically excited-states of conjugated molecules.

Contrary to their ground-state counterparts, excited-states are short-lived, highly reactive and often coupled together, making the quest to master them a capital but extremely challenging task. In fact, even accurate and extensive descriptions of the ground-state properties, fell short to understand the behaviours of electronically excited compounds. In that framework, accurate theoretical models delivering a characterisation of the elemental electron processes are actively searched for to define strategies useful for the design of novel compounds with tailored properties. Aiming to optimise excited-state properties of medium and large conjugated compounds, Time-Dependent Density Functional Theory (TD-DFT) developed 25 years ago by Runge and Gross [6–16], is certainly a very popular model. Indeed, it provides a rapid, yet often accurate, description of the excited-state properties for both gas-phase and solvated molecules, and is able to tackle large problems. Despite its successes and versatility, TD-DFT suffers from a major limitation: the quality of the results depends significantly on the selected functional, and the dependence between these functional and the obtained accuracy remains the subject of intense discussions [17–19]. For this reason, it is usually necessary to benchmark the approach to ensure its adequacy for the specific chromogen

* Corresponding author.
E-mail address: Denis.Jacquemin@univ-nantes.fr (D. Jacquemin).

0143-7208/$ – see front matter © 2011 Elsevier Ltd. All rights reserved.
doi:10.1016/j.dyepig.2011.07.016

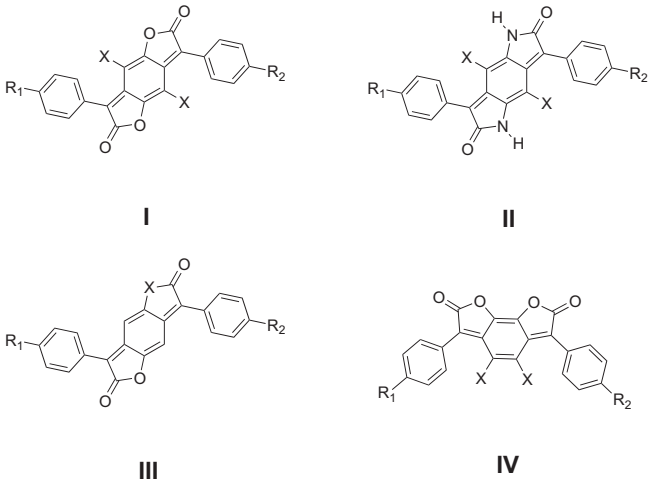

Fig. 1. Representation of the experimental structures under investigation.

under investigation, and such assessment will be performed here before analysing the excited-state nature and testing strategies to optimise the properties of the benzodifuranone derivatives. To the best of our knowledge, there is only one previous theoretical work aiming at the simulation of excite-state properties of this family, but it was "limited" to unsubstituted symmetric **I** and **II** and their position isomers [20]. Indeed, Ref. [20] is focussed on the evolution of the properties when the chromophore lengthens, that is Lunak's paper deals with systems containing several (rather than one) central phenyl rings and does not tackle the impact of chemical substitution. Subsequently, the present investigation constitutes the first contribution aiming to an accurate estimation of auxochromic effects for this series. We strive for a fast, easy-to-use, yet accurate computational protocol.

This paper is organised as follows: in Section 2 we describe the general computation procedure, in Section 3 we present and discuss our main results in 4 subsections, devoted to benchmark, comparison with experiment, push–pull effects and potential DSSC dyes. Eventually, the main conclusions arising from our investigation are discussed in Section 4.

2. Method

All simulations have been performed with the Gaussian 09 program [21], with a tighten self-consistent field convergence threshold (10^{-8} to 10^{-10} a.u). We have followed a well-established three-step approach [13]: (i) the ground-state geometry of each dye has been optimised until the residual mean force is smaller than 1.0×10^{-5} a.u; (ii) the vibrational spectrum is analytically determined to confirm that the structure is a true minimum; and (iii) the vertical transition energies to the valence excited-states are computed with a linear-reponse TD-DFT approach, using a vertical approximation. These vertical values are straightforwardly compared to the experimental λ_{max}, which is a common approximation for large structures. Several basis sets and functionals have been tested for each steps and the results are presented in the following Section. The bulk solvent effects were evaluated using the Polarisable Continuum Model (PCM) [22], that is able to obtain a valid approximation of solvent effects as long as no specific interactions link the solute and the solvent molecules. Because we simulate absorption spectra, we have turned on the non-equilibrium linear-response PCM solutions [23], since the absorption processes typically present short characteristic times. In the following the representation of the molecular orbitals has been performed using a contour threshold of 0.03 a.u.

3. Results and discussion

3.1. Methodological investigation

To the best of our knowledge, there is no previous investigation aiming at an accurate simulation of the optical properties of benzodifuranone dyes, and we have begun by setting up such a method. To this end, complete benchmark have been performed for ubsubstituted dyes **I** and **II** (that is $R_1 = R_2 = R_3 = X = H$ in Fig. 1) starting with a "standard" TD-PBE0/6-31+G(d)//PBE0/6-31G(d) model [24], and testing all components of this approximation. Though compulsory, this part of the work is not the most appealing to non-expert and we present only a brief overview here, Tables-collating all numerical data are given in Supplementary material.

For the geometries, no XRD of structures closely related to benzodifuranone could be found in the CSD database. Therefore, we have applied wavefunction approaches, up to MP4(SDQ) [fourth-order Møller–Plesset with single, double and quadruple excitations], so to obtain accurate benchmark data for our DFT simulations (Table S1). For π-conjugated molecules, it is known that the "truth" [e.g. highly-correlated approaches] is in between MP2 (second-order Moller–Plesset) and MP4(SDQ), but is closer to the former [25]. Consequently, we can discard both the Hartree–Fock approach that yields too localised values and pure DFT schemes that suffer from the opposite drawback. All tested hybrids, namely B3LYP [26], PBE0 [24], M06-2X [27] and CAM-B3LYP [28], provide sound estimates but for slightly too short carbonyl bond lengths (error of ca. −0.01 Å) and an underrated twist angle between the benzodifuranone core and the side phenyl rings (ca. −5° underestimation). PBE0 has been selected in the following, as this functional provides a λ_{max} nicely matching the above MP2/MP4(SDQ) criterion. In a second step, a basis set investigation was performed for the geometry (Table S2). The largest basis sets yield consistent data for all distances as well as for the transition wavelength computed at the TD-PBE0/6-31+G(d) level, indicating that convergence has been reached. Whilst double-ζ basis set overshoot the λ_{max} by ca. 10 nm, 6-311G(d,p) appears as a good compromise between accuracy and efficiency. Indeed, it provides negligible errors for the geometrical parameters (<0.005 Å for bond lengths) and discrepancies limited to ca. 3–4 nm for the λ_{max}.

For both dyes, the impact of increasing the basis set size on the estimated spectrum is limited once the geometry has been fixed, as can be seen in Table S3 of Supplementary material. Indeed, even the tiny 6-31G is close to the spot but this outcome probably originates from error compensations between the lack of polarisation and diffuse orbitals. The first basis set providing nearly converged values for both unsubstituted **I** and **II** is 6-311+G(2d,p) and this basis set has been applied for all subsequent calculations. Experimentally, the measured λ_{max} are 466 nm for **I** in chloroform and 452 nm for **II** in dimethylformamide (DMF) [1]. Before comparing to experiment, it is legitimate to estimate the impact of environmental effects. With the PCM model, we found that going from gas-phase to chloroform (DMF) implies a bathochromic shift of +36 nm (+26 nm) for **I** (**II**), a variation mainly ascribable to the TD part of the calculation. Solvatochromism should therefore be accounted for and the functional benchmarks listed in Table S4 have been performed applying the PCM continuum model during both the geometry optimisation and excited-state simulations. As expected [18], pure functionals lead much too small transition energies and TD-HF is also inadequate. Amongst the hybrids, the smallest errors

Table 1
Comparison between theoretical and experimental λ_{max} (in nm). Type refers to the naming conventions given in Fig. 1. All theoretical values have been obtained at the PCM-TD-DFT/6-311+G(2d,p)//PCM-PBE0/6-311G(d,p) level of approximation.

Dye				Solvent	Theory			Experiment	
Type	R_1	R_2	X		M06-2X	CAM-B3LYP	ωB97XD	λ_{max}	Ref.
I	H	H	H	$CHCl_3$	471	476	477	466	[1,2]
	H	H	Cl	$CHCl_3$	459	464	462	457	[1,2]
	H	H	Me	Toluene	435	440	440	428	[1]
	Cl	NHPr	H	Toluene	589	592	585	628	[3]
	H	NHMe	H	Toluene	575	578	571	606	[3]
	H	OMe	H	$CHCl_3$	505	512	507	498	[2]
	Me	Me	H	DMF	491	497	494	486	[4]
	NEt_2	NEt_2	Br	Pyridine	687	683	661	726	[2]
	OCOMe	OCOMe	H	DMF	480	486	484	475	[1]
	OH	OH	H	Acetone	517	523	518	523	[1,2]
	OMe	OMe	Cl	$CHCl_3$	526	531	523	536	[1,2]
II	H	H	H	DMF	461	465	465	452	[1,2]
III	H	H	NCOMe	$CHCl_3$	472	478	478	459	[2]
	Me	Me	NCOMe	$CHCl_3$	492	498	496	482	[2]
	H	H	S	$CHCl_3$	471	477	477	470	[2]
	OMe	OMe	S	$CHCl_3$	535	540	536	523	[2]
IV	H	H	H	Toluene	485	490	492	474	[2]
	OMe	OMe	Cl	Toluene	537	542	537	540	[2]

are obtained with M06-2X [27], CAM-B3LYP [28] and ωB97XD [29] that all yield errors smaller than 15 nm as well as a sound shift between the two dyes. The fact that two range-separated hybrid and a global hybrid including a larger share of exact exchange emerge as the most efficient are typical of electronic transitions implying a significant electronic rearrangement [17,30], a fact confirmed in Section 3.3.

In short, we have selected a PCM-TD-DFT/6-311+G(2d,p)//PCM-PBE0/6-311G(d,p) model for the following, and pre-selected three functionals for the TD part: M06-2X, CAM-B3LYP and ωB97XD. Of course, this selection has been made in a pragmatic (cost/efficiency) way, i.e. more refined excitation or solvent models could have lead different results. Indeed, we compare vertical TD-DFT values to experimental λ_{max}, a physically-incorrect, yet popular approach. More physically-sound comparisons of 0–0 values are nevertheless difficult due to, on the one hand, the absence of a large set of experimental data (often only λ_{max} are listed) and, on the other hand, the large computational cost related to computation of vibrationally-resolved spectra. Typically, there is a ca. 0.2 eV difference between the vertical and 0–0 energies at the TD-DFT level [31–33]. For solvation, there exists a refined but more costly state-specific approach [34], that is available in Gaussian 09 and allows to account for the polarisation of the cavity at the excited-state. Using this model for (unsubstituted) benzodifuranone, we reached a sizable −27 nm variation in chloroform with M06-2X. It should therefore be clear to the reader that the "best" functional for the TD part is also related to the selection of vertical linear-response approximations.

3.2. Comparison between theoretical and experimental spectra

Table 1 compares the absorption spectra computed with the three functionals to their experimental counterparts for a set of eighteen dyes possessing a core closely related to the benzodifuranone chromogen. This panel of molecules includes both symmetric and asymmetric dyes, mixes mild and strong auxochromic groups, as well as several polar and apolar solvents. When possible, we have selected aprotic solvent in such a way that the PCM model, that does not include specific solvent–solute interactions, remains fully valid. Note that, in one case (**III** with X = S), it was necessary to convolute the theoretical spectra with a broadening Gaussian (0.4 eV FWHM) due to the presence of two intense transitions, close in energy, in the theoretical TD-DFT stick spectrum. Nevertheless, for most dyes, TD-DFT reveals only one strongly dipole-allowed transition in the visible domain of the electromagnetic spectra, which is consistent with the fact that experimental paper generally reports only one band [1–3], hinting that the next absorption is in the UV domain.

The auxochromic effects are reasonably reproduced. For instance, for unsubstituted **I**, adding a Cl (Me) group in X induces an hypsochromic shift of −9 nm (−38 nm), and M06-2X foresees −12 nm (−36 nm). The same holds for stronger electroactive groups: plugging NEt_2 moieties at both R_1 and R_2 gives a +260 nm variation, an important qualitative effect reproduced with the correct order of magnitude, though slightly undershot by M06-2X (+216 nm), as well as by the two range-separated hybrids (CAM-B3LYP: +207 nm ωB97XD: +184 nm). Likewise in **IV**, adding both methoxy and chlorine side groups provokes a measured bathochromic displacement of +66 nm, whereas M06-2X, CAM-B3LYP and ωB97XD predict variations of +52 nm, +52 nm and +45 nm, respectively.

The first striking conclusion obtained from a statistical analysis is that all three functionals provide alike values. Indeed, the typical deviations between the three hybrids are as small as 5 nm. The agreement with experimental data is also quite astonishing, with mean signed errors (MSE, experiment-theory) of 2.3 nm, −2.4 nm

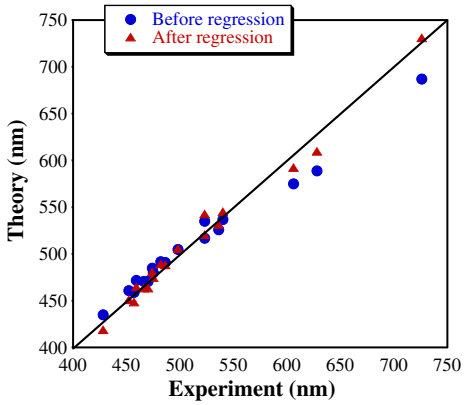

Fig. 2. Comparison between M06-2X and experimental wavelengths prior and after correction by a simple linear regression. The central line indicates a perfect match between theory and experiment.

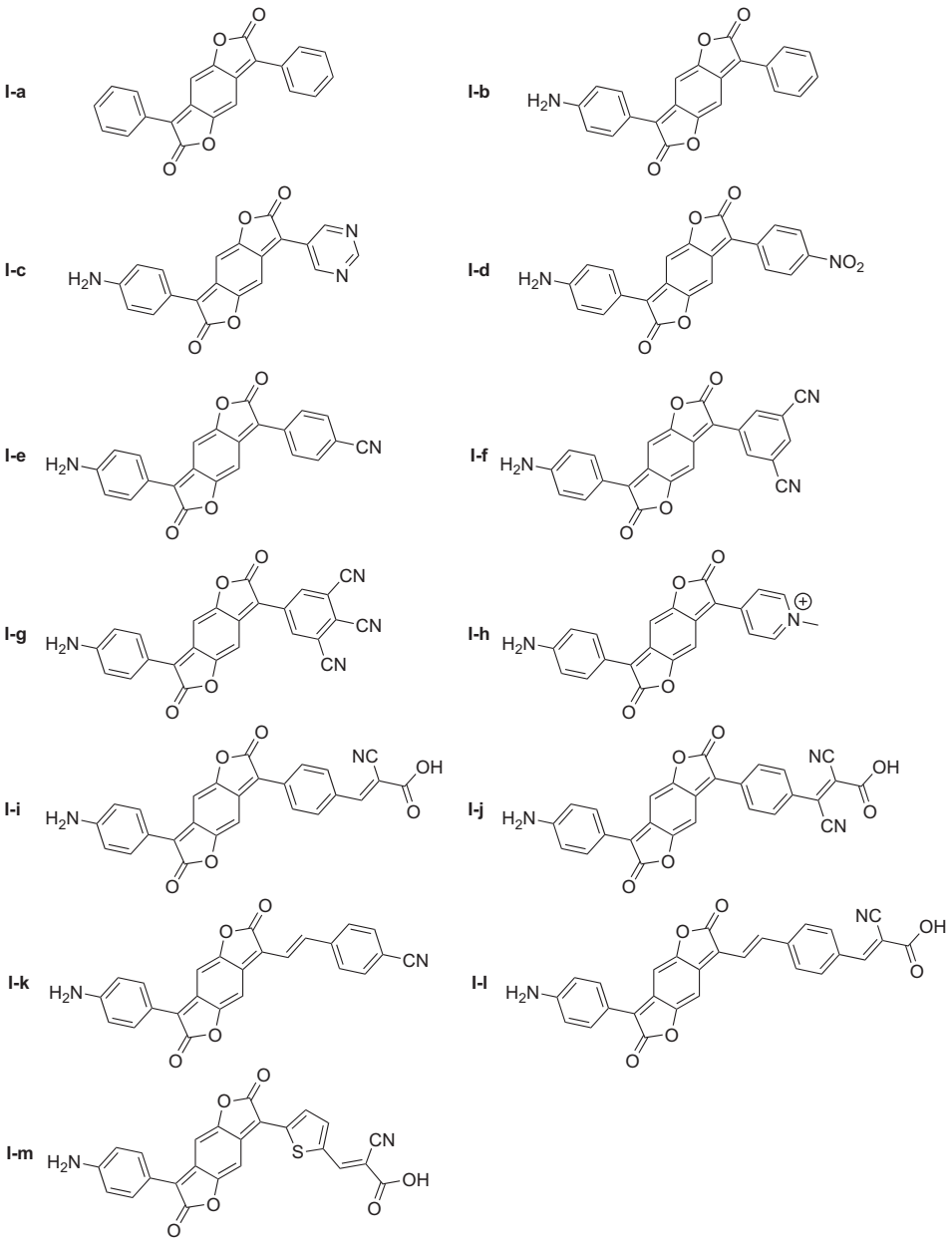

Fig. 3. Push–pull dyes investigated.

and 1.4 nm for M06-2X, CAM-B3LYP and ωB97XD, respectively. The corresponding mean absolute errors (MAE) are 12 nm, 15 nm and 17 nm, respectively. Linear regressions performed on the full set of dyes listed in Table 1 yield three correcting equations:

$$\lambda^{\mathrm{corr}} = -119.42 + 1.24\lambda^{\mathrm{M06-2X}} \quad (1)$$

$$\lambda^{\mathrm{corr}} = -145.88 + 1.28\lambda^{\mathrm{CAM-B3LYP}} \quad (2)$$

$$\lambda^{\mathrm{corr}} = -201.04 + 1.40\lambda^{\omega\mathrm{B97XD}} \quad (3)$$

that are associated with very large R^2: 0.985, 0.984 and 0.981, for M06-2X, CAM-B3LYP and ωB97XD, respectively. The corresponding MAE are 7.0 nm, 7.4 nm and 8.1 nm, confirming that M06-2X is the most efficient of the three functionals both before and after linear regression. This agreement is well illustrated in Fig. 2 that confirms

Table 2
Computed absorption wavelengths (nm) in toluene for a series of benzodifuranone dyes of Fig. 3. We list both the raw and corrected (Eq. (1)) values, together with the computed oscillator strength. At the right hand side, the energies of the HOMO and LUMO are given in eV.

Molecule	$\lambda^{\mathrm{M06-2X}}$	λ^{corr}	f	H	L
I-a	472	466	1.47	−7.32	−3.15
I-b	548	560	1.40	−6.73	−3.00
I-c	562	576	1.35	−6.87	−3.20
I-d	578	596	1.47	−6.89	−3.28
I-e	571	588	1.48	−6.87	−3.23
I-f	579	597	1.41	−6.95	−3.33
I-g	612	639	1.54	−7.05	−3.57
I-h	671	711	1.50	−7.85	−4.55
I-i	592	618	1.75	−6.83	−3.29
I-j	600	623	1.70	−6.86	−3.37
I-k	602	626	1.93	−6.68	−3.23
I-l	628	653	2.26	−6.65	−3.29
I-m	655	691	1.91	−6.73	−3.46

that the "raw" values already provide an accurate description of the major chemical effects.

Let us briefly discuss solvatochromic effects. For **I** with R_1 = Cl and R_2 = NHPr (R_1 = H and R_2 = NHMe), we computed with M06-2X, solvatochromic shifts of +4 and +5 nm (+15 and +16 nm) when going from toluene to acetone and ethanol, respectively. These values include both geometric and electronic effects, that is the geometries and spectra have been computed in each solvents. The corresponding experimental values are +8 and +26 nm (+21 and +33 nm), so that theory reasonably reproduces the sign and amplitude of the effect for acetone but is not very accurate for ethanol, an expected outcome for an

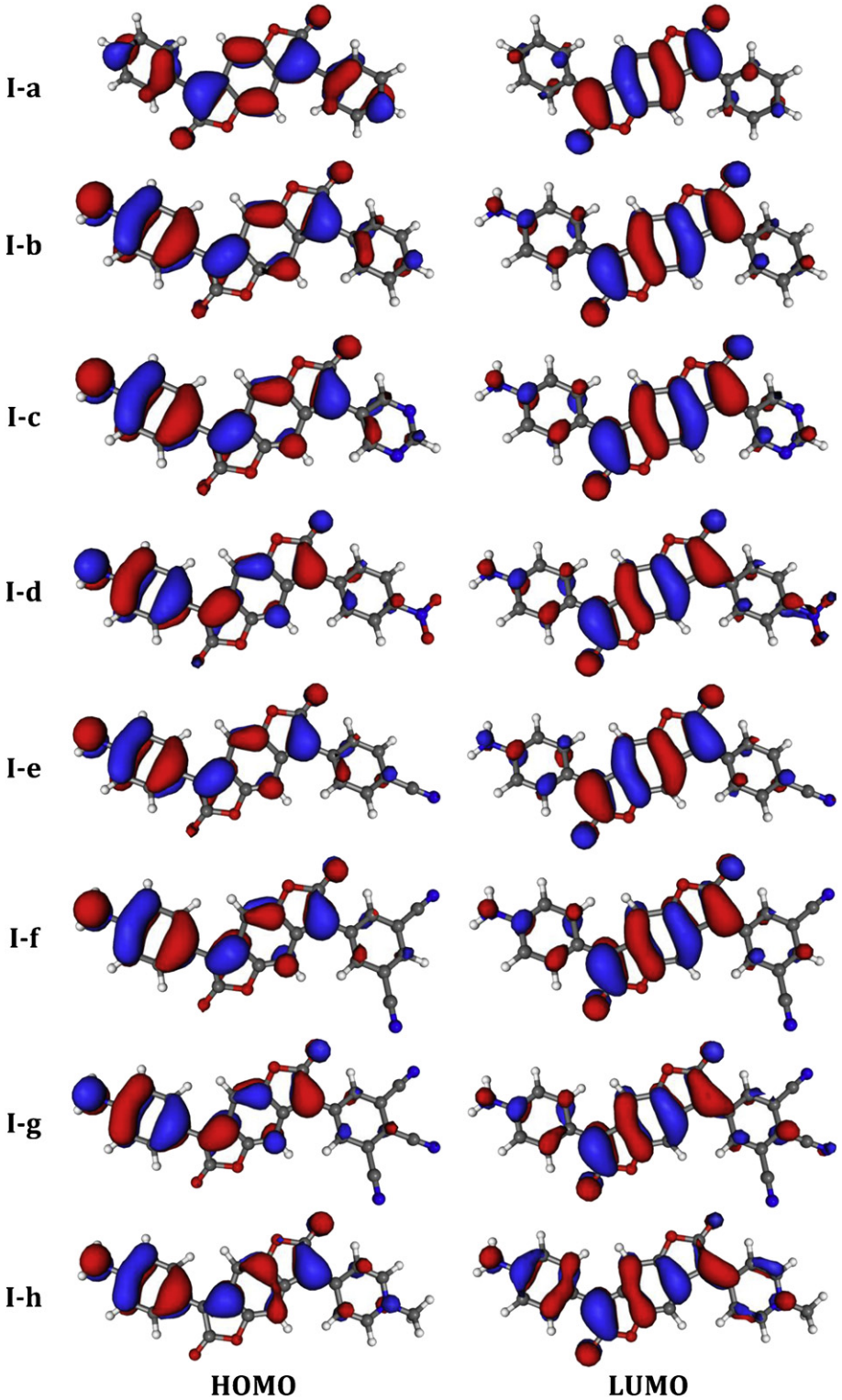

Fig. 4. Topology of the frontier orbitals for the eight top dyes of Fig. 3. These orbitals have been computed at the PCM-TD-M06-2X/6-311 + G(2d,p)//PCM-PBE0/6-311G(d,p) level, using a contour threshold of 0.03 a.u.

hydrogen-bond donor solvent that is less adequately modeled by a continuum solvation model.

According to these results, all three selected functionals are adequate to reproduce the auxochromic effects, though M06-2X has a slight edge and is consequently used in the following.

3.3. Analysis of the nature of excited-states

Having an efficient computational protocol at hand, we have studied several new structures. These compounds are represented in Fig. 3, the numerical results being summarised in Table 2. For the unsubstituted **I-a**, the absorption band computed at 472 nm (in toluene) presents a very large oscillator strength ($f = 1.47$) and almost exclusively implies an HOMO (highest occupied molecular orbital) to LUMO (lowest unoccupied molecular orbital) electronic promotion. This latter conclusion actually holds for all dyes of Fig. 3 which eases the analysis. The topology of the frontier orbitals of **I-a** are displayed in Fig. 4. The HOMO is delocalised over the full molecule with major contributions on the double bonds of the benzodifuranone as well as on the side phenyl rings, whereas the LUMO is mainly located on the single bonds of the central core. In other words, the electronic absorption presents the expected $\pi \rightarrow \pi^*$ nature and implies a partial electron transfer from the periphery to the centre of the dye.

A popular strategy to induce a large bathochromic shift is to add one strong donor group (e.g. amine) and one strong acceptor group (e.g. cyano) on two opposite sides of the molecule, so to simultaneously increase the energy of the HOMO and decrease the energy of the LUMO. This so-called push–pull scheme is efficient for most classes of conjugated dyes and has been tested for the benzodifuranones (see Table 2). Adding a NH_2 group at R_1 (**I-b**) yields the expected effect with a +94 nm bathochromic shift and a sharp surge of the HOMO (+0.59 eV). Fig. 4 confirms that the HOMO is now asymmetric and implies the aniline side, whereas the LUMO is mostly unchanged compared to **I-a**. On the contrary, typical acceptors like pyrimidine, nitro and cyano groups (**I-c**, **I-d** and **I-e**) have a smaller impact than foreseen: they increase the λ_{max} by a quite disappointing ~20 nm and only slightly stabilise the LUMO (ca. −0.25 eV, less than half of the amine-induced variation though one would expect a cooperative effect). If one aims to induce a large bathochromic shift, adding donor groups on the benzodifuranone core is therefore a more efficient strategy than adding accepting groups, that have a weak impact. This is in the line of experiment (see previous Section with the very large NEt_2 auxochromic effect) and is also consistent with the topologies of the frontier orbitals of the three (**I-c**, **I-d** and **I-e**) dyes. Indeed, they possess almost exactly the same LUMO as the unsubstituted molecule, and do not display the characteristic features of the electron-accepting groups (Fig. 4). The hallmark acceptor orbitals lay higher in energy (typically the LUMO+1 for these dyes). Therefore, we have heighten the pulling strength by using two (**I-f**) or three cyano (**I-g**) groups as well as the positively charged pyridinium (**I-h**), the latter being a considerably strong accepting moiety. The two latter dyes undergo significant bathochromic shift compared to **I-b**: +79 nm and +151 nm for **I-g** and **I-h**, respectively. For the pyridinium, the variation of the LUMO energy becomes sizeable (>1 eV) but at the price of a significant (undesired) stabilisation of the HOMO, due to the presence of a positive charge that reduces the Coulombic repulsions. In fact, the LUMO of **I-h** is not strongly perturbed compared to **I-a**: the contributions on the two side phenyl rings are significant but far from dominating. The twist angle between the benzodifuranone core and the pyridinium ring is limited to 10°, and this outcome

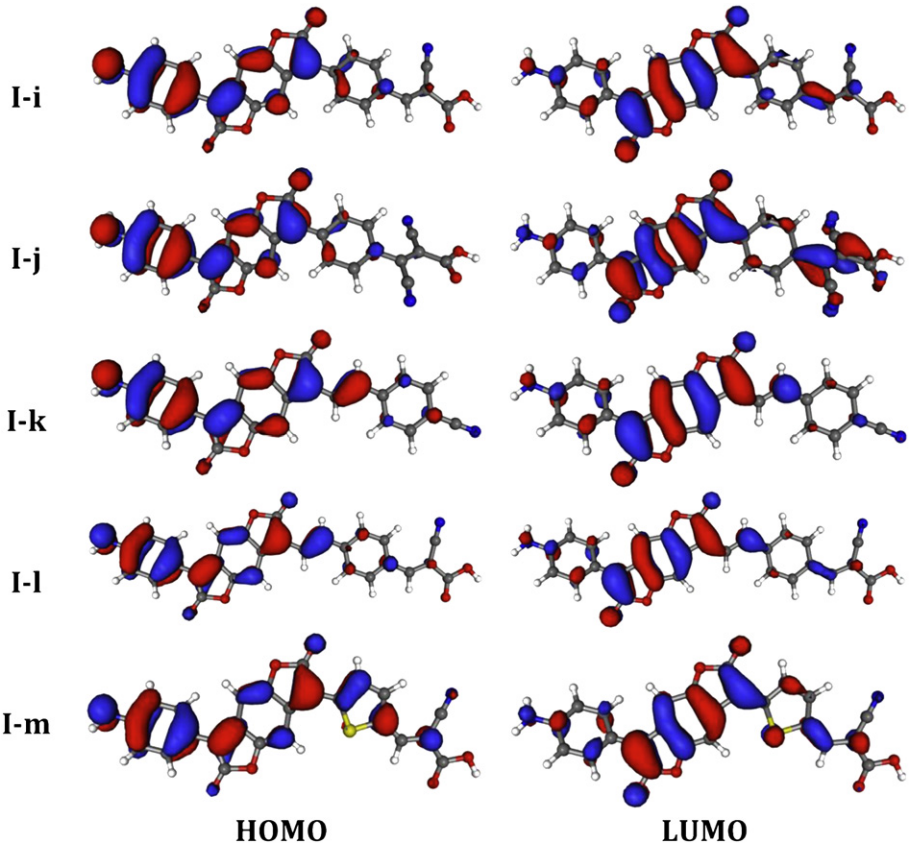

Fig. 5. Topology of the frontier orbitals for the five bottom dyes of Fig. 3. See caption of Fig. 4 for more details.

does not originate in a lack of electronic communication between the two moieties.

In short, we have shown that the benzodifuranone core acts like a strong acceptor at the excited-state, i.e. presents a very stable LUMO. Indeed, only the pyridinium is able to significantly perturb it.

3.4. Potential for DSSC dyes

Before investigation "realistic" DSSC dyes, we have performed calculations on model systems, conserving the NH_2 donor, but varying the opposite side with substituents closer to typical anchoring functions, such as cyanoacetic terminal group (bottom five dyes in Fig. 3). The results are collated in Table 2, the corresponding representation of the frontier molecular orbitals can be found in Fig. 5. For **I-i** and the stronger **I-j**, one notices relatively modest bathochromic shift and LUMO stabilisation compared to **I-b**. For the latter, the contribution on the anchoring group that bears two cyano acceptors become significant, though the major component of the LUMO density remains located on the benzodifuranone core. To increase the communication, we have added an ethenyl moiety (**I-k** and **I-l**) or replaced one phenyl ring by thiophene, all structures showing nearly planar geometries in this side

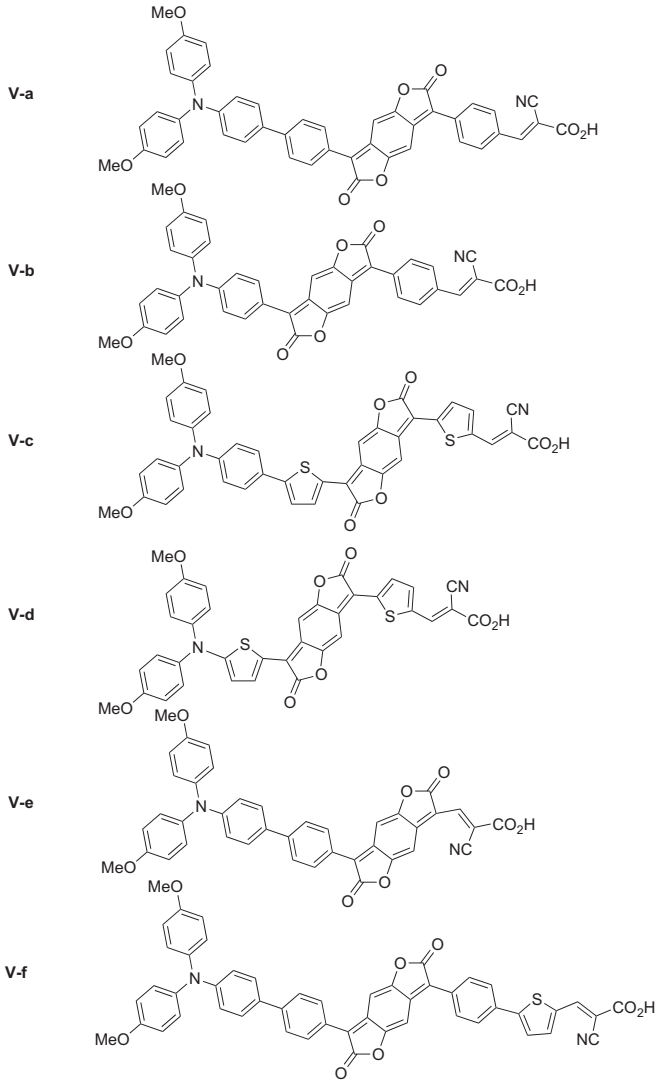

Fig. 6. Potential DSSC dyes.

Table 3
Computed absorption wavelengths (nm) in toluene for a series of potential DSSC dyes (Fig. 6). See caption of Table 2 for more details.

Molecule	$\lambda^{M06\text{-}2X}$	λ^{corr}	f	H	L
V-a	641	675	1.42	−6.27	−3.40
V-b	679	721	1.82	−6.41	−3.30
V-c	824	901	2.12	−6.23	−3.57
V-d	797	868	2.05	−6.23	−3.37
V-e	770	846	1.31	−6.36	−3.81
V-f	622	651	1.70	−6.25	−3.29

of the molecule. The latter presents the most significant bathochromic shift (predicted λ_{max} of 691 nm) and the LUMO is partly delocalised on the thiophene and vicinal double bond, but to a rather limited extend, if one target electron transfer.

In Fig. 6, we represent six dyes potentially useful for DSSC applications. They have been designed using a triarylamine donor and a rod-like architecture, clearly following previous theoretical and experimental works relying on other central chromophores (e.g. oligothiophene, diketopyrrole…) [35–38]. Indeed, one can hope that a stronger donor group would help improving the charge-transfer character of the system. We are well aware that the semi-conductor might have a strong impact on the properties of the dyes [39,40], and that the present investigation on isolated structures may only provide first insights. The obtained results are displayed in Table 3, the simulated spectra in Fig. 7 and the frontier orbitals in Fig. 8. Note that for the dyes presenting very large λ_{max}, the corrected values with Eq. (1) should be considered cautiously, so that Fig. 7 uses raw TD-DFT results. It clearly turns out that the double thiophene dyes, **V-c** and **V-d** present the smallest transition energies, with foreseen absorptions in the near IR, whereas more traditional patterns (**V-c**) absorbs at smaller wavelength, indicating a tunable λ_{max}. By inspecting the HOMO and LUMO of Fig. 8, one notices that the HOMO is localised on the donor group (but for **V-d**) and that the LUMO is centered on the benzodifuranone, as expected from the results of the previous Section. Therefore, a desired left-to-right electron transfer may take place, but unfortunately, not towards the anchoring moiety, but for **V-e** that may be the most promising of the series. For several dyes, there are several absorption bands (see Fig. 7) some being located in a valuable domain for harvesting natural light, e.g. 522 nm ($f = 0.58$) for **V-e**. However, these bands also imply transitions towards the LUMO, so that the above analysis remains adequate. Other parameters are important for obtaining efficient DSSC dyes, e.g. the injection speed into the semi-conductor, the photostability of the structures and the ability to be reduced by the iodine redox couple. Though most

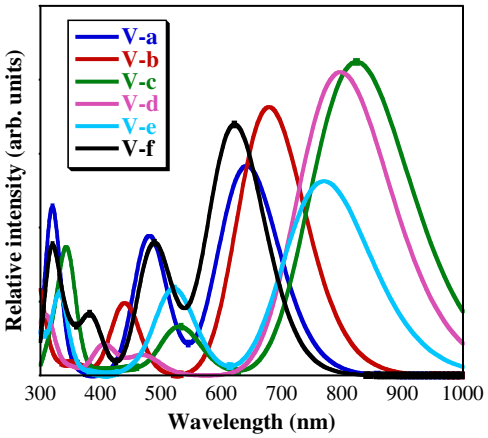

Fig. 7. Simulated spectra (0.35 eV FWHM Gaussian used) for the dyes of Fig. 6.

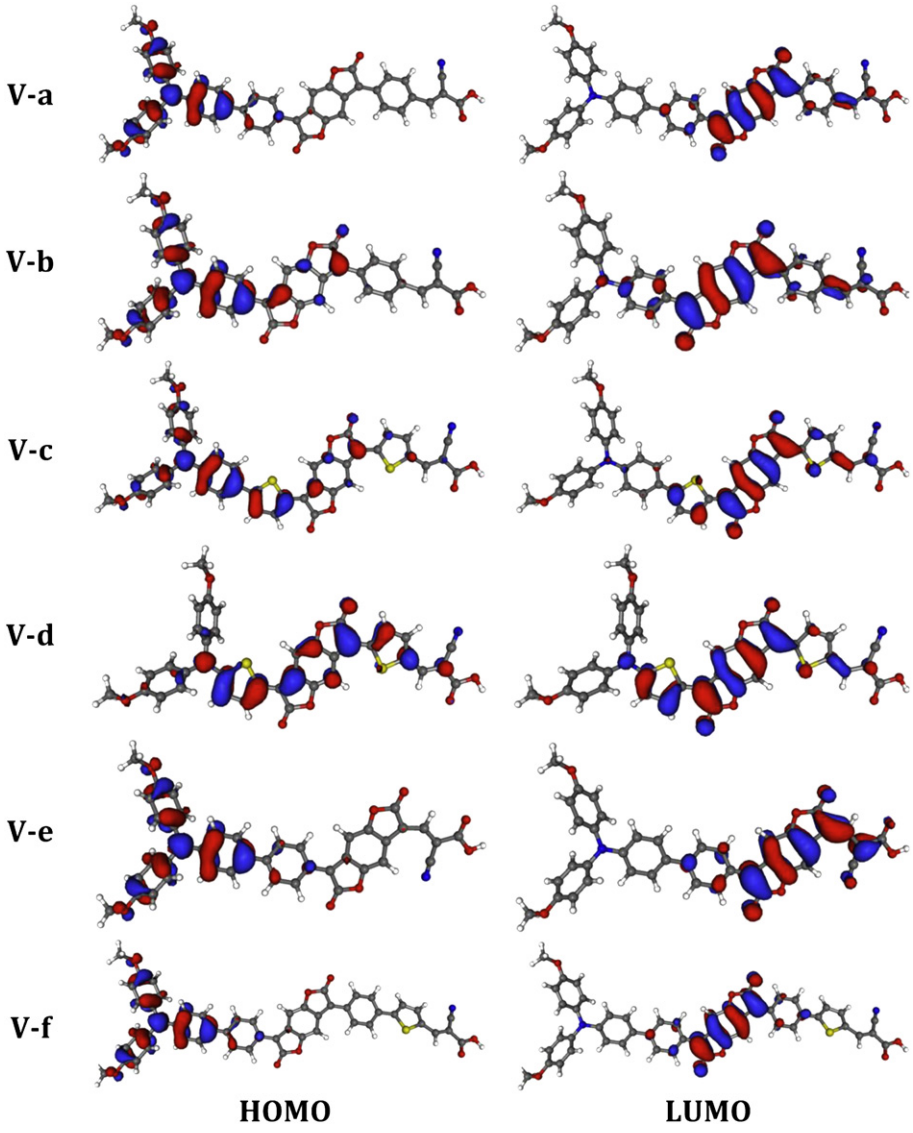

Fig. 8. HOMO and LUMO of DSSC dyes.

benzodifuranone derivatives do not fit all desired optical and charge-transfer requirements, let us briefly discuss these points. There is no general approach to estimate photostability with theoretical tools, but asymmetric benzodifuranones present an excellent light-fastness [2], hinting that resistance to incoming photons should not be a major issue. On the contrary, the regeneration of benzodifuranone dyes would probably be an issue, as we computed very stable LUMO level. To gain more insights, we have used the same level of theory to investigate dyes in which the diketopyrrolopyrrole group replaces the benzodifuranone core and the obtained LUMO are ca. 1.5 eV less stable (~ -2.0 eV instead of -3.5 eV, see Table 3). As the regeneration of diketopyrrole dyes is already a practical limit [36], one can conclude that benzodifuranone is apparently not the best fragment for DSSC applications. The same qualitative reasoning holds for electron injection: the LUMO of the benzodifuranone is so stable that fast injection is far from guaranteed [39].

4. Conclusions

We have performed a theoretical investigation striving for both a reliable prediction of the λ_{max} of benzodifuranone derivatives and an optimisation of their properties in the framework of DSSC dyes. We have tested several computational models, and the PCM-TD-M06-2X/6-311+G(2d,p)//PCM-PBE0/6-311G(d,p) emerged has a powerful computational protocol able to provide accurate and converged description for both the geometrical and optical parameters. Indeed, for a set of 18 dyes for which theory/experiment comparison is straightforward, we obtained a mean absolute error as small as 12 nm, a discrepancy that can further be reduced by a factor of two when a simple linear regression is applied. An analysis of the topology of the frontier orbitals playing a role in the visible transition shows that the HOMO can be lifted by using conventional donor groups, whereas the LUMO, centred on the benzodifuranone core, can only be tuned by the most powerful acceptors (pyridinium). Consequently, if one aims to use a benzodifuranone containing dyes in DSSC, the only possible strategy is to locate this chromophore as close as possible from the ZnO or TiO_2 surface so to ensure a non-trifling orbital mixing with the bands of the surface. Nevertheless, such purpose-designed molecule might remain inefficient due to the low-energy of the LUMO that may impede electron injection and induces difficulties to regenerate the dye with the redox mediator. Methods aiming to circumvent these drawbacks are currently under investigation in Nantes.

Acknowledgement

J.P.C.-C. acknowledges the Région des Pays de la Loire and the fellowship provided by the Fundación Séneca, Agencia de Ciencia y Tecnología de la Región de Murcia, within its Postdoctoral Research Staff Training Program. D.J. is indebted to the Région des Pays de la Loire for financial support in the framework of a recrutement sur poste stratégique. The work was partially supported by the Fundación Séneca del Centro de Coordinación de la Investigación de la Región de Murcia under Project 08735/PI/ 08, and by the Ministerio de Educación y Ciencia of Spain under Projects CTQ2007-66528 and CONSOLIDER CSD2009-00038. This research used resources of the GENCI-CINES/IDRIS (Grant c2011085117) and of the CCIPL (Centre de Calcul Intensif des Pays de Loire). This work was partly supported by the ANR HABISOL (program Asyscol, n°ANR-08-HABISOL-002).

Appendix. Supplementary material

Supplementary material related to this article can be found online at doi:10.1016/j.dyepig.2011.07.016.

References

[1] Greenhalgh CW, Carey JL, Newton DF. The synthesis of quinodimethanes in the benzodifuranone and benzodipyrrolidone series. Dyes Pigm 1980;1:103–20.
[2] Greenhalgh CW, Carey JL, Newton DF. The benzodifuranone chromogen and its application to disperse dyes. J Soc Dyers Colour 1994;110:178–84.
[3] Hallas G, Yoon C. The synthesis and properties of red and blue benzodifuranones. Dyes Pigm 2001;48:107–19.
[4] Cai Z, Gao J, Li X, Xiang B. Synthesis and characterization of symmetrical benzodifuranone compounds with femtosecond time-resolved degenerate four-wave mixing technique. Opt Commun 2007;272:503–8.
[5] A SciFinder (CAS) database search yield numerous patents, e.g. CN-102031017 (2011) WO-2011020789 (2010), CN-101983993 (2010), CN-101899229 (2010); 2011.
[6] Runge E, Gross EKU. Density-functional theory for time-dependent systems. Phys Rev Lett 1984;52:997–1000.
[7] Casida ME. Time-dependent density-functional response theory for molecules. In: Recent advances in density functional methods, vol. 1. Singapore: World Scientific; 1995. pp. 155–92.
[8] Stratmann RE, Scuseria GE, Frisch MJ. An efficient implementation of time-dependent density-functional theory for the calculation of excitation energies of large molecules. J Chem Phys 1998;109:8218–24.
[9] Perdew JP, Ruzsinsky A, Tao J, Staroverov VN, Scuseria GE, Csonka GI. Prescription for the design and selection of density functional approximations: more constraint satisfaction and fewer fits. J Chem Phys 2005;123:062201.
[10] Dreuw A, Head-Gordon M. Single-reference ab initio methods for the calculation of excited states of large molecules. Chem Rev 2005;105:4009–37.
[11] Barone V, Improta R, Rega N. Quantum mechanical computations and spectroscopy: from small rigid molecules in the gas phase to large flexible molecules in solution. Acc Chem Res 2008;41:605–16.
[12] Casida ME, Jacquemin D, Chermette H. Time-dependent density-functional theory for molecules and molecular solids. J Mol Struct (Theochem) 2009; 914:1–2.
[13] Jacquemin D, Perpète EA, Ciofini I, Adamo C. Accurate simulation of optical properties in dyes. Acc Chem Res 2009;42:326–34.
[14] Biczysko M, Panek P, Barone V. Toward spectroscopic studies of biologically relevant systems: vibrational spectrum of adenine as a test case for performances of long-range/dispersion corrected density functionals. Chem Phys Lett 2009;475:105–10.
[15] Quartarolo AD, Sicilia E, Russo N. On the potential use of squaraine derivatives as photosensitizers in photodynamic therapy: a tddft and ricc2 survey. J Chem Theory Comput 2009;5:1849–57.
[16] Quartarolo AD, Russo N. A computational study (tddft and ricc2) of the electronic spectra of pyranoanthocyanins in the gas phase and solution. J Chem Theory Comput 2011;7:1073–81.
[17] Peach MJG, Benfield P, Helgaker T, Tozer DJ. Excitation energies in density functional theory: an evaluation and a diagnostic test. J Chem Phys 2008;128: 044118.
[18] Jacquemin D, Wathelet V, Perpète EA, Adamo C. Extensive td-dft benchmark: singlet-excited states of organic molecules. J Chem Theory Comput 2009;5: 2420–35.
[19] Goerigk L, Grimme S. Assessment of td-dft methods and of various spin scaled cis$_n$d and cc2 versions for the treatment of low-lying valence excitations of large organic dyes. J Chem Phys 2010;132:184103.
[20] Lunak S, Vynuchal J, Hrdina R. Dft and td dft study of isomeric benzodifuranones, benzodipyrrolinones and their analogues. J Mol Struct 2009;935: 82–91.
[21] Frisch MJ, Trucks GW, Schlegel HB, Scuseria GE, Robb MA, Cheeseman JR, et al. Gaussian 09 revision A.02. Wallingford CT: Gaussian Inc.; 2009.
[22] Tomasi J, Mennucci B, Cammi R. Quantum mechanical continuum solvation models. Chem Rev 2005;105:2999–3094.
[23] Cossi M, Barone V. Time-dependent density functional theory for molecules in liquid solutions. J Chem Phys 2001;115:4708–17.
[24] Adamo C, Barone V. Toward reliable density functional methods without adjustable parameters: the pbe0 model. J Chem Phys 1999;110:6158–70.
[25] Jacquemin D, Adamo C. Bond length alternation of conjugated oligomers: wave function and dft benchmarks. J Chem Theory Comput 2011;7:369–76.
[26] Becke AD. Density-functional thermochemistry. 3. the role of exact ex-change. J Chem Phys 1993;98:5648–52.
[27] Zhao Y, Truhlar DG. The m06 suite of density functionals for main group thermochemistry, thermochemical kinetics, noncovalent interactions, excited states, and transition elements: two new functionals and systematic testing of four m06-class functionals and 12 other functionals. Theor Chem Acc 2008; 120:215–41.
[28] Yanai T, Tew DP, Handy NC. A new hybrid exchange-correlation functional using the coulomb-attenuating method (cam-b3lyp). Chem Phys Lett 2004; 393:51–6.
[29] Chai JD, Head-Gordon M. Long-range corrected hybrid density functionals with damped atom–atom dispersion corrections. Phys Chem Chem Phys 2008;10:6615–20.
[30] Jacquemin D, Perpète EA, Ciofini I, Adamo C, Valero R, Zhao Y, et al. On the performances of the m06 family of density functionals for electronic excitation energies. J Chem Theory Comput 2010;6:2071–85.
[31] Furche F, Ahlrichs R. Adiabatic time-dependent density functional methods for excited states properties. J Chem Phys 2002;117:7433–47.
[32] Dierksen M, Grimme S. The vibronic structure of electronic absorption spectra of large molecules: a time-dependent density functional study on the influence of exact Hartree–Fock exchange. J Phys Chem A 2004;108:10225–37.
[33] Jacquemin D, Brémond E, Planchat A, Ciofini I, Adamo C. Td-dft vibronic couplings in anthraquinones: from basis set and functional bench-marks to applications for industrial dyes. J Chem Theory Comput 2011;174:1882–92.
[34] Improta R, Barone V, Scalmani G, Frisch MJ. A state-specific polarizable continuum model time dependent density functional theory method for excited state calculations in solution. J Chem Phys 2006;125:054103.
[35] Preat J, Michaux C, Jacquemin D, Perpète EA. Enhanced efficiency of organic dye-sensitized solar cells: triphenylamine derivatives. J Phys Chem C 2009; 113:16821–33.
[36] Qu S, Wu W, Hua J, Kong C, Long Y, Tian H. New diketopyrrolopyrrole (dpp) dyes for efficient dye-sensitized solar cells. J Phys Chem C 2010;114:1343–9.
[37] Pastore M, Fantacci S, De Angelis F. Ab initio determination of ground and excited state oxidation potentials of organic chromophores for dye-sensitized solar cells. J Phys Chem C 2010;114:22742–50.
[38] Yu S, Ahmadi S, Zuleta M, Tian HN, Schulte K, Pietzsch A, et al. Adsorption geometry, molecular interaction, and charge transfer of triphenylamine-based dye on rutile tio2(110). J Chem Phys 2010;133:224704.
[39] Labat F, Ciofini I, Hratchian HP, Frisch MJ, Raghavachari K, Adamo C. First principles modeling of eosin-loaded zno films: a step toward the understanding of dye-sensitized solar cell performances. J Am Chem Soc 2009;131: 14290–8.
[40] Le Bahers T, Labat F, Pauporté T, Lainé PP, Ciofini I. Theoretical procedure for optimizing dye-sensitized solar cells: from electronic structure to photovoltaic efficiency. J Am Chem Soc 2011;133:8005–13.